Nephrol Dial Transplant (2008) 23: 3752–3761
doi: 10.1093/ndt/gfn470
Advance Access publication 9 September 2008

Editorial Review

NDT
Nephrology Dialysis Transplantation

BK virus large T and VP-1 expression in infected human renal allografts

Christian A. Seemayer[1], Norbert H. Seemayer[2], Ursula Dürmüller[1], Fred Gudat[1], Stefan Schaub[3], Hans H. Hirsch[4] and Michael J. Mihatsch[1]

[1]Institute for Pathology, University Hospital Basel, Schönbeinstrasse 40, CH-4003 Basel, Switzerland, [2]Institute of Virology, University Hospital Essen, Hufelandstrasse 55, D-45122 Essen, Germany, [3]Clinic for Transplantation Immunology and Nephrology, University Hospital Baseland and [4]Transplantation Virology, Medical Microbiology, University of Basel, CH-4003 Basel, Switzerland

Abstract

Objective. We investigated the expression of early and late phase BK virus (BKV) proteins and their interactions with host cell proteins in renal allografts, with ongoing polyomavirus associated nephropathy (PVAN), and correlated this with the nuclear and cell morphology.

Methods. Frozen sections from three patients with renal allografts (two biopsies, one explant) with PVAN were analysed by indirect immunofluorescence using BKV specific anti-polyoma large T-antigen and anti-VP-1 antibodies, as well as anti-p53, anti-Ki67, anti-caspase-3, anti-bcl2 and anti-cytokeratin 22 antibodies. Nuclear morphology and size were estimated by DNA Hoechst staining.

Results. In infected tubular cells the early and late phases of infection could be distinguished according to expression of large T-antigen or VP-1. The early phase revealed almost normal nuclear proportions, whereas in later phases nuclear size increased about 2 to 3 fold. Expression of large T-antigen was strongly associated with accumulation of p53 in the nucleus, accompanied by the activation of the cell cycle associated cell protein Ki67. In contrast, expression of BKV VP1 correlated only weakly with p53. Virus dependent cell lysis was due to necrosis, since neither caspase 3 nor nuclear nor cytoskeleton changes indicated apoptosis.

Conclusion. In our selected patients with PVAN a clear distinction between early and late phases was possible, according to the protein expression patterns of BKV markers. Striking nuclear enlargement is only present in the late phase of infection. In the inflammatory setting of PVAN, BKV dependent effects appear to be mediated by the inhibition of p53, resulting in the activation of the cell cycle. We assume that in PVAN similar BKV mechanisms are operative as in certain *in vitro* systems.

Keywords: BK virus nephropathy; renal transplantation

Correspondence and offprint requests to: Michael J. Mihatsch, Institute for Pathology, University Hospital Basel, Schönbeinstrasse 40, CH-4003 Basel, Switzerland. Tel: +41-61-265-2872; Fax: +41-61-265-3194; E-mail: mjmihatsch@uhbs.ch

Introduction

The BK virus (BKV) is a human polyomavirus first isolated from the urine of a kidney transplant patient with ureteric stenosis [1]. A decade ago, BKV received renewed attention as a candidate of human disease and emerged as the principal agent of polyomavirus-associated nephropathy (PVAN) [2–5] eliciting severe dysfunction of renal allografts with progressive graft loss in >90% of cases [5–7]. The emergence of PVAN among kidney transplants coincided with the widespread use of potent immunosuppressive drugs such as tacrolimus and mycophenolate mofetil, thus implicating severely impaired antiviral immunity as a critical factor [8].

In the course of disease, initially, so-called decoy cells, i.e. urothelial or tubular cells with virus inclusion bodies, are present in the urine. Later, renal biopsies show viral cytopathic changes in tubular cells, tubular cell necroses, interstitial inflammation and finally interstitial fibrosis. The definitive diagnosis of PVAN depends on characteristic cytopathic changes such as intranuclear inclusions in tubular epithelial cells and/or detection of BKV large T antigen by immunohistochemistry [3,6,9].

In vitro, the phases of the BKV infectious cycle [10,11] and the interaction of viral proteins with host cell proteins have been studied. However, *in vivo* and specifically in human renal allografts with ongoing BKV nephropathy, cross-talk between the virus and infected cell has not been systematically addressed. Whether *in vitro* and *in vivo* phases are similar is an open question; in this respect the majority of *in vitro* studies focused on the transforming effects of BKV. A better understanding of the *in vivo* BKV infectious cycle in PVAN may be of interest for making a more precise diagnosis.

In the present study, we investigated the expression of early (large T-Ag) and late (VP-1) BKV proteins in frozen biopsy sections of a selected group of patients with ongoing BKV nephropathy by immunofluorescence (IF) and compared this with expression of host cellular proteins, such as the tumour suppressor protein p53, the cell

Table 1. Clinical parameters of our three patients with renal transplants and ongoing BKV nephropathy corresponding to stages A, B and C

Variable	Stage A	Stage B	Stage C
Recipient			
Sex	Female	Female	Female
Age	65	36	55
Donor			
Living donor	Yes	No	Yes
Age	38	7	56
HLA-mismatches	2	3	4
Initial immunosuppression	Sir-MMF-P	ATG-Tac-MMF-P	ATG-CyA-Aza-P
Parameters at the time of biopsy			
Time post-transplant	5 months	3 months	12 months
Immunosuppressive therapy	Tac-MMF-P	Tac-MMF-P	Tac-P
Creatinine (μmol/L)	216	179	On haemodialysis
BK-viraemia (copies/mL)	6.4×10^4	2.8×10^6	2.5×10^6
Decoy cells (per 10 HPF)	133	534	Positive

ATG = polyclonal anti-T-lymphocyte globulin; CyA = cyclosporine A; Tac = tacrolimus; Sir = sirolimus; MMF = mycophenolate-mofetil; Aza = azathioprine; P = prednisone; HPF = high power field.

Table 2. List of primary antibodies that were used in the present study

Name of antibody	Clone	Species	Type	Recognized antigen	Dilution	Incubation period (h)	Company/ reference	Positive controls
Anti-SV40 large T-antigen	PAb 416	Mouse	Monoclonal	Large T-ag of SV40 and BKV	1:20	1	Oncogene, San Diego, CA, USA	SV40-transformed RASF[a]
Anti-VP1	–	Rabbit	Polyclonal	VP1 of BKV	1:200	2	Hirsch *et al.* [9]	WB[b]
Anti-VP1	–	Mouse	Monoclonal	VP1 of BKV	1:100	1	Gordon J., Temple University, Philadelphia, USA	WB[b]
Anti-p53	–	Rabbit	Polyclonal	Human p53	1:25	1	Epitomics, Burlingame, CA, USA	Bladder carcinoma
Anti-Ki67	NCL-Ki67p	Rabbit	Polyclonal	Ki 67	1:100	1	Novacastra, Newcastle, UK	Tonsil
Anti-Ki67	MIB-1	Mouse	Monoclonal	MIB-1/Ki67	1:100	1	DAKO, Glostrup, DK	Tonsil
Anti-caspase 3	–	Rabbit	Polyclonal	Human/mouse active caspase 3	1:20	1	R&D Systems, Minneapolis, MN, USA	Tonsil
Anti-bcl-2	–	Rabbit	Polyclonal	Bcl-2	1:100	1	Santa Cruz, distr. by Labforce, Nunningen, CH	Tonsil
Anti-CK22	–	Mouse	Monoclonal	Human cytokeratin cocktail CK22	1:10	1	Biomeda, Foster City, CA, USA	All epithelial cells positive

[a]SV40-transformed rheumatoid arthritis synovial fibroblasts (RASF, Seemayer *et al*., 2003) [12].
[b]Anti-VP1 antibodies are not commercially available. Specificity was tested by western blotting (WB).

cycle-associated protein Ki67, the cytokeratin CK22, the apoptosis marker caspase 3 and the anti-apoptotic protein bcl-2. From these data we estimated the time course of the viral infectious cycle *in vivo* and the type of virus-dependent cell death.

Materials and methods

In the present study, two biopsies and one explanted kidney allograft from three patients, representing the three different stages of PVAN, were studied by light microscopy in paraffin and by IF in frozen tissue sections. All tissue samples were sufficiently large, each containing >10 glomeruli and several clusters of tubules with infected cells. Cases were selected due to their amount of frozen tissue available in order to perform a large panel of double-labelling IF investigations. The clinical parameters of the patients are presented in Table 1.

Snap frozen tissue sections (5 μm) were air dried and fixed at room temperature with perjodate-lysine-paraformaldehyde or acetone (for detection of bcl-2). Consecutively, fixed sections were analysed by indirect IF in single and double labelling techniques, utilizing the following antibodies (Tables 2 and 3).

For detection of the following antigens, the controls indicated were used: (1) p53—urothelial bladder carcinoma, (2) bcl-2 and caspase-3-–T-lymphocytes in tonsilar tissue undergoing apoptosis or expressing bcl-2 and (3) SV40—transformed synovial fibroblasts [12].

As negative controls, we utilized concentration-adjusted non-specific mouse or rabbit IgG to replace the primary antibody.

Table 3. Summary of double labelling experiments with mouse or rabbit antibodies in appropriate combinations

	Anti-p53 rabbit	Anti-Ki67 rabbit	Anti-Ki67 mouse	Anti-CK22 mouse	Anti-Casp. 3 rabbit	Anti-Bcl-2 rabbit	Anti-VP1 rabbit
Anti-large T-Ag mouse	+	+	−	−	+	+	+
Anti-VP1 mouse (rabbit)	+	−	+ (Rabbit)	+ (Rabbit)	+	+	+

Double labelling was performed by (i) application of mouse monoclonal antibodies and consecutive staining with Cy3-labelled goat anti-mouse antibodies (red fluorescence), and (ii) administration of rabbit polyclonal or monoclonal antibodies was followed by the 2nd anti-rabbit $F(ab)_2$ fragments labelled with Alexa 488 (green fluorescence). With each double labelling, single staining for each marker was performed on parallel sections.

Stained sections were analysed with a Zeiss fluorescence microscope at a magnification of 250-fold. Overlay of the red, green and blue IF staining was performed with an online video camera (Hammamatsu), adding each signal separately. The resulting pictures were evaluated on the video screen at a 400-fold magnification and afterwards digitalized using the KS300 program.

Quantification of the signals

Three autopsy kidneys without any abnormalities were stained with Hoechst dye 33258, and the nuclear density of all cells present was counted in six high-power fields of the renal cortex. On average, in the cortex 79 (±12) and in the medulla 95 (±4), tubular nuclei were found, resulting in a mean number of nuclei of 87 per HPF. This number was taken to roughly estimate the maximum number of signals that could be obtained in one area of interest.

Since PVAN typically occurs in clusters, only positive areas were evaluated by counting 10 HPF per slide, positioning the affected tubulus in the centre of the HPF. To overcome slide-dependent differences in expression, two to five parallel sections were analysed and the data were pooled (Table 4). The standard deviation (SD) indicates the variability between parallel sections. The expression of BKV large T-antigen and VP1 was correlated with nuclear size measuring the numbers of pixels per nucleus. Double-labelled sections were assessed for nuclear size and expression of viral markers utilizing the KS300 program. On digitalized pictures specific nuclei were replaced by white colour and the number of pixels in the region of interest was determined. More than 100 nuclei per specimen were analysed and the results categorized as (a) no BKV protein expression, (b) expression of large T-antigen only, (c) double labelling of large T-antigen and VP1 and (d) single staining of VP1 protein.

Results

Characterization of cases with BKV nephropathy

Three cases representing the different stages of PVAN [13] were used (Table 1). The biopsy corresponding to stage A (early/initial PVAN) revealed an early involvement of the medulla (Figure 1A). The tubular cell lesions were so minor that the definite diagnosis was only made after SV40 staining; inflammation and necrosis were minimal. The biopsy of stage B (florid) showed marked viral lesions in the cortex and medulla, necrosis and prominent inflammation, but little tubular atrophy and fibrosis (Figure 1B). The nephrectomy specimen showed end-stage PVAN (stage C: late sclerosing) with viral lesions in cortex and medulla, extensive tubular cell necrosis, minor inflammation and most severe interstitial fibrosis and tubular atrophy (Figure 1C).

Table 4. Absolute numbers of positive cells for BKV and host cell protein markers. For three patients (stages A–C) with renal transplants and ongoing BKV nephropathy at least two up to five parallel sections for each marker were analysed

Marker[a] (number of sections)	Stage A	Stage B	Stage C[c]
Anti-large T-Ag, mouse ($n = 5$)	63.4 ± 7.1	49.6 ± 16.9	51.4 ± 16.9
Anti-VP-1, rabbit ($n = 3$)	45 ± 7.2	28.7 ± 7.5	58 ± 30.5
Anti-VP-1, mouse ($n = 2$)	34 ± 12.7	28 ± 5.7	65 ± 30.4
Anti-p53, rabbit ($n = 2$)	35 ± 9.9	32.5 ± 30.4	32.5 ± 17.7
Anti-Ki67, rabbit/mouse ($n = 2$)[b]	63.5 ± 21.9	117 ± 15.5	98.5 ± 12.0
Anti-caspase 3, rabbit ($n = 2$)	0	0	0
Anti-bcl-2, rabbit ($n = 2$)	0	0	0
Anti-CK22, mouse ($n = 2$)	All	All	All
Hoechst 33258	All	All	All

[a]Positive cells ± SD in randomly selected 10 high-power fields (HPF). Total number of cells/10 HPF ∼850.
[b]Data of the mouse and rabbit anti-Ki67 antibodies were pooled, because of staining overlap of >95%.
[c]Kruskall Walllis test: no significant differences were found between the groups.

By immunofluorescence (IF), per single section, on average 50–60 large T-antigen positive tubular epithelial nuclei per 10 HPF could be detected (Table 4). Ten HPF corresponded in average to 850 nuclei resulting in 6–7% infected cells in the analysed clusters. VP1 antigens were detected in the nucleus and also in the cytoplasm. In stage C of PVAN, the number of VP1 positive cells was slightly higher than in the two other biopsies corresponding to stages A and B, but did not reveal statistical significance. Accumulation of VP1 was associated with enlarged nuclear size and altered nuclear shape (see below). In addition, and more pronounced in the graft nephrectomy specimen (stage C), cellular debris and tubular casts stained extensively for the VP1 protein, most likely indicating release of BKV virions from lysed cells.

The tumour suppressor protein p53 was expressed on average in 33 of the nuclei per 10 HPF in all three patients,

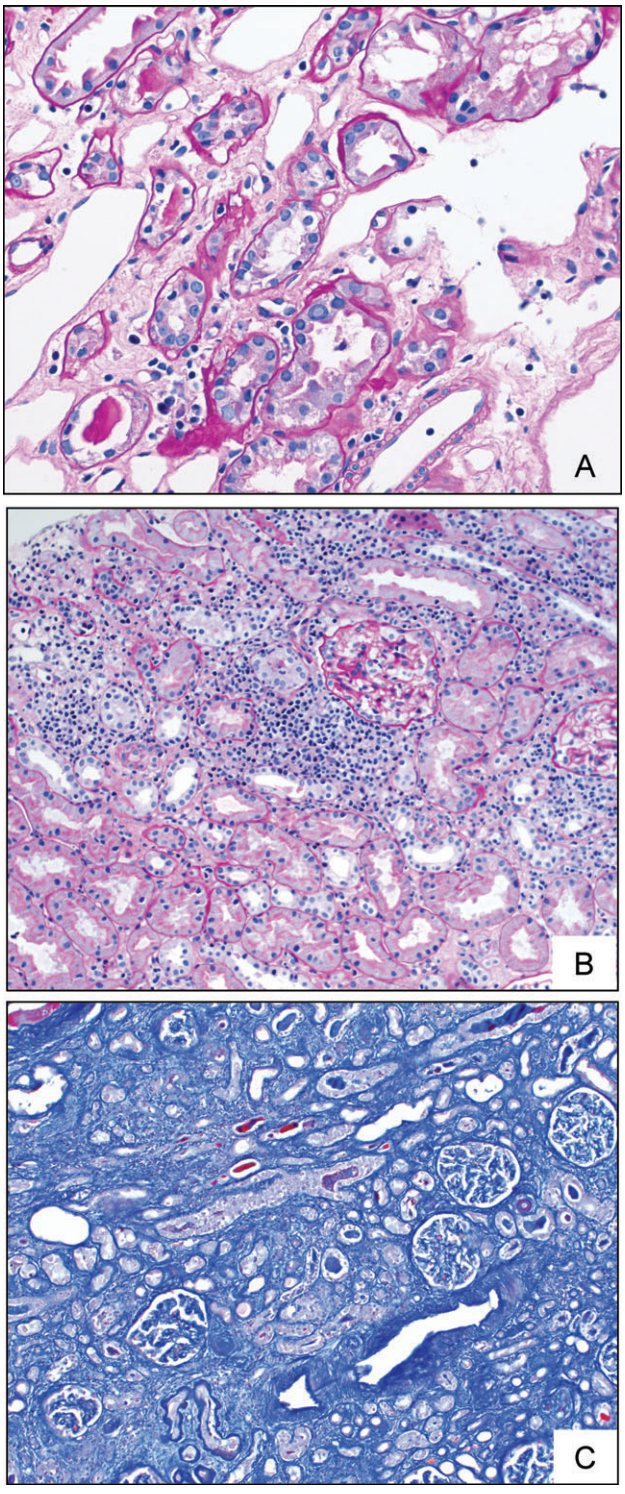

Fig. 1. Histology of our three patients (A, B, C) with ongoing PVAN in the corresponding stages A, B and C. (**A**) (Patient A): cortico-medullary junction: tubules with cells showing typical inclusion bodies. In the corresponding frozen sections much more infected cells were present than in the paraffin sections. PAS stain, original magnification 400×. (**B**) (Patient B): cortex with focal inflammation surrounding tubules with infected cells. PAS stain, original magnification 200×. (**C**) (Patient C): cortex with severe interstitial fibrosis and tubular atrophy. In-between better preserved areas of cortical tissue. Trichrome stain, original magnification 100×.

whereas the cell cycle-associated protein Ki67 was present in 100–120 nuclei per 10 HPF in the cases of stages B and C, but was lower in stage A, with only 64 positive nuclei.

Staining for the apoptosis marker caspase 3 and the anti-apoptotic protein bcl-2 was negative in tubular cells; tonsil tissue served as a positive control, with specific signals in lymphocytes. However, bcl-2 was expressed in inflammatory cells adjacent to infected tubuli (Figure 2). The cytokeratin CK22 was strongly expressed in all tubular epithelial cells and the Hoechst dye 33258 showed a regular distribution of nuclear DNA, thereby indicating lack of apoptosis.

Co-expression of large T-antigen with the tumour-suppressor protein p53 and the cell cycle-associated protein Ki67

Expression of large T-antigen was strongly associated with accumulation of p53 in the nucleus (Figure 2A and B). In 70% (± 0.5%) of T-antigen positive nuclei, a complete overlay with p53 in the nucleus was seen. In 96% of the cells found to express p53, T-antigen was also co-localized, indicating a strong co-expression of T-antigen and p53 *in vivo*, which is known to be mediated by binding and stabilization.

The cell cycle-associated protein Ki67 was less strongly associated with the expression of T-antigen than p53. On average ∼60% of T-antigen expressing nuclei also contained the Ki67 protein, but, in contrast to p53, no complete overlay of the two staining patterns in the nucleus was seen. Ki67 positive cells were twice as frequent as T-antigen expressing cells, and >60% of Ki67 positive cells did not co-stain for T-antigen. These cells revealed smaller nuclei than those co-expressing the large T-antigen and most likely correspond to non-BKV-infected cells.

Co-expression of large T-antigen with the virus capsid protein VP1

In the biopsy tissue samples (patients A and B, stages A and B), large T-antigen was expressed twice as frequently as VP1 (Figure 2C and D). In contrast, in patient C (stage C), VP1 expression dominated twofold, suggesting that most of BKV replication was in the late phase. However, irrespective of which BKV protein was dominant, expression of the early phase protein large T and the late phase virus capsid protein VP1 was virtually exclusive. Eighty percent of T-antigen positive cells did not co-stain for the VP1 protein. The remaining 20% of double-stained cells revealed only a partial overlay of these proteins, indicating both a time- and space-dependent separation of expression *in vivo*, as has been described *in vitro*.

Co-expression of the virus capsid protein VP1 with p53 and Ki67

Expression of the virus capsid protein was loosely associated with accumulation of p53 in the nucleus (Figure 2C and D). Only 29% of VP1 positive cells expressed p53; a partial overlay in terms of the cellular compartment was seen. The level of co-expression between VP1 and p53

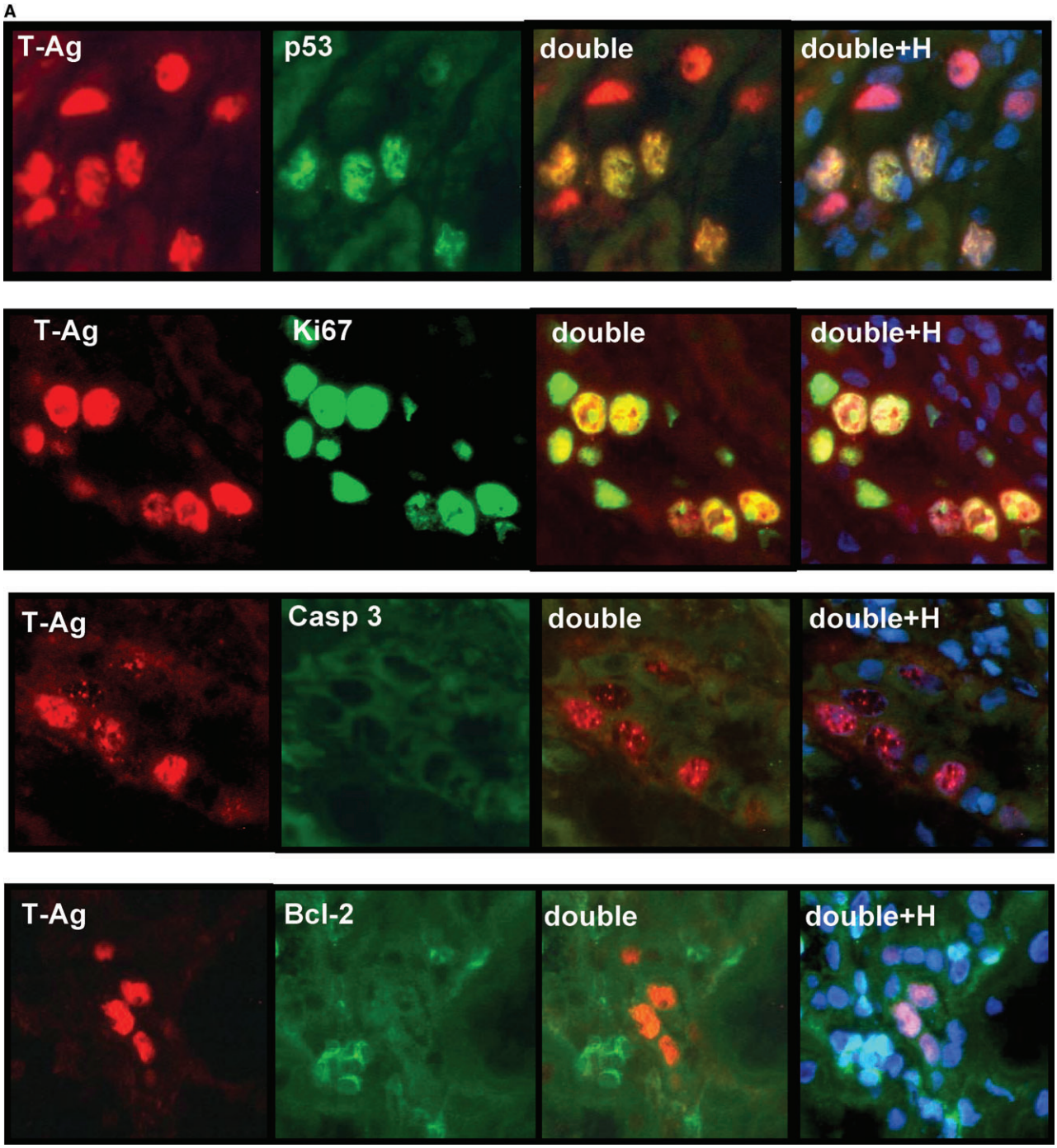

Fig. 2. Investigation of the expression of large T-antigen and VP1 BKV proteins and their interaction with host cell proteins by immunfluorescence (IF) double labelling techniques in kidney transplanted patients with ongoing PVAN. The IF images are taken from patient B (Figure 1a and c), and the quantifications of the results includes all three patients (Figure 1b and d). (**A**) Double labelling of large T-antigen with p53, Ki67, caspase 3 and Bcl-2 in single, double or triple channels including the DNA staining of the nuclei by Hoechst (H) dye in blue. In a double channel, overlay of the red and green signal results in an orange-yellow colouration. (**B**) Quantification of the number of cells expressing large T-antigen and co-localizing p53, Ki67, caspase 3 and Bcl-2. The numbers of T-antigen expressing cells is adjusted to 1 (=100%). Bars indicate the standard deviation (SD) between the three patients. (**C**) Double labelling of VP1 with large T-antigen, Ki67, p53 and caspase 3 in single, double or triple channels. In addition, DNA is stained by Hoechst (H) dye in blue. Co-expression of the red and green signal causes an orange-yellow colouration. (**D**) Quantification of the number of cells expressing VP1 and co-localizing large T-antigen, Ki67, p53 and caspase 3. The numbers of VP1 expressing cells are adjusted to 1 (=100%). Bars indicate the SD between the three patients.

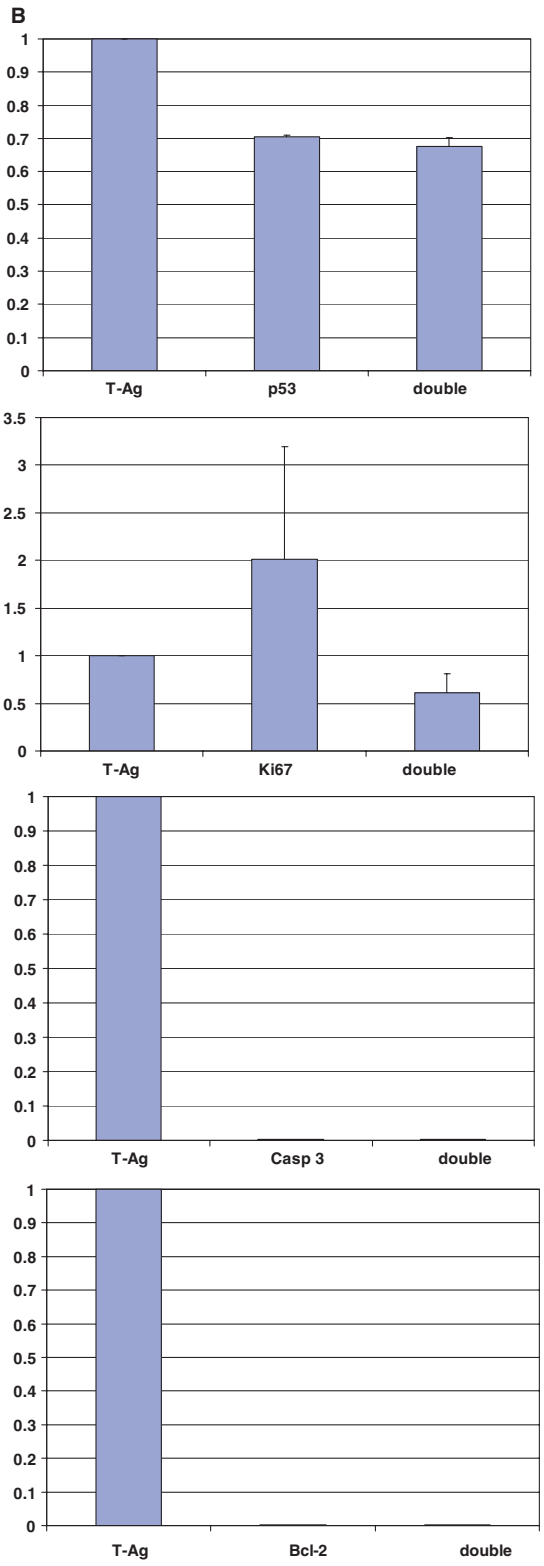

Fig. 2. (*Continued*).

was ∼10% higher than the co-expression of VP1 and T-antigen, indicating that p53 might be expressed slightly longer within the virus cycle than T-antigen, or that T-antigen binding to p53 was no longer required for p53 expression in this late phase.

The cellcycle-associated protein Ki67 was co-expressed in 50% of the VP1 positive cells. However, Ki67 signals were threefold more frequent than VP1 signals, such that 70% of the Ki67 expressing cells were VP1 negative. In line with the results from the T-antigen and Ki67 studies, the majority of Ki67 expressing cells was negative for viral antigens and probably corresponds to repopulating tubular epithelial cells, without any virus replication.

Co-expression of early and late phase BKV proteins correlates with nuclear size

BKV-antigen negative tubular epithelial cells revealed ∼1293 pixels (± SEM 46) per nucleus, whereas nuclei expressing the large T-antigen were significantly increased in size by ∼30% (1676 pixels ± 124) (Figure 3). Nuclei staining positive for VP1 were ∼70% larger (2427 pixels ± 201), compared to those solely expressing large T-antigen. The size of the large T/VP1 double-stained nuclei (3722 pixel ± 387) was about threefold and the VP1 positive cells about twofold larger, in comparison to control cells. The nuclear size of the different cell types was significantly different from each other [analysis of variance: at least ($P < 0.03$)].

Accordingly, nuclear size increases with the course of the virus infection and reaches a maximum upon expression of VP1 and T-antigen in the early replication phase. The decrease in the nuclear size of cells lacking detectable large T-antigen expression, but expressing VP1, could be due to uneven nuclear distribution of both antigens, particularly in the very late phase, with partial release of BK virion.

Investigation of co-expression BKV proteins with the apoptosis marker active caspase 3, the anti-apoptotic protein bcl2 and the cytokeratin CK22

The apoptosis marker activated caspase 3 could not be detected in tubular epithelial cells in any of the tissue specimens examined, but was positive in the appropriate positive controls. In addition, Hoechst dye staining of DNA revealed neither nuclear shrinkage nor apoptotic bodies. In line with the lack of apoptotic tubular epithelial cells, strong expression of the cytokeratin CK22 was observed in the BKV-positive cells. No signs of degradation of cytoskeleton proteins were seen, as would be the case with ongoing apoptosis. The anti-apoptotic protein bcl-2 was also absent in virus-infected tubular cells, but was readily detectable in lymphocytes adjacent to the virus-infected tubuli.

Discussion

Expression of early and late phase BKV proteins and their interaction with host cell proteins was examined in tissue specimens from three renal transplant patients in three different stages with ongoing PVAN.

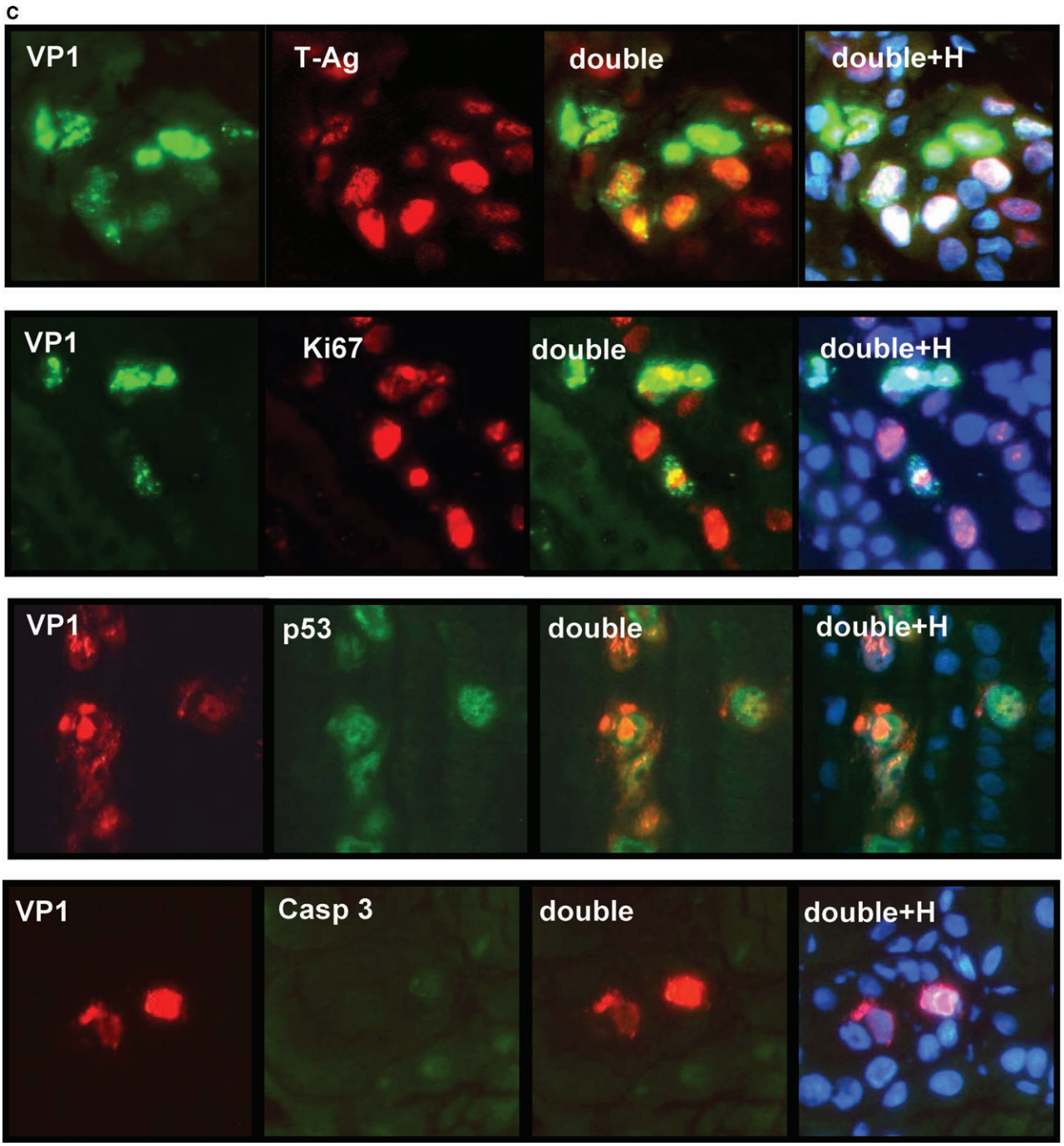

Fig. 2. (*Continued*).

Specifically, our data show the following:

(1) Infection of the kidney transplants with BKV occurs in our group of investigated patients in clusters, but infected cells are in different phases of the virus cycle in one and the same tubule and in different tubules. In the *in vivo* situation of PVAN in each cell, a clear distinction between early and late phase infection can be made according to the expression of large T-antigen or VP1. The early phase is associated with nearly normal nuclear size and shape, but in later phases nuclear size increases dramatically, by about two- to threefold, when the nuclear cross-section area is evaluated.

This is fully in line with the recent *in vitro* data obtained from BKV infection in primary cultures of human tubular kidney epithelial cells and demonstrating a clear distinction of early and late phase [11]. The expression of VP1 correlated strongly with the viral DNA replication, thereby indicating the late phase. These data confirm earlier studies—already performed three decades ago [14,15] investigating BKV replication in monkey-derived

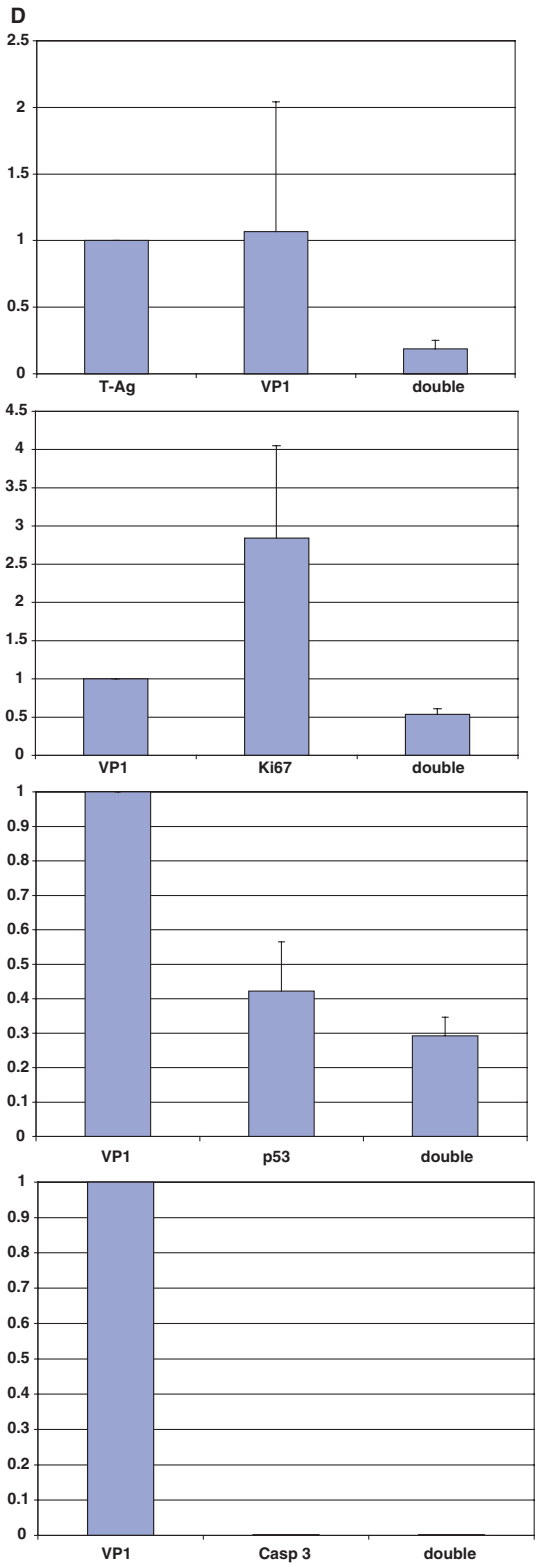

Fig. 2. (*Continued*).

kidney cells (Vero), in human a embryonic kidney cell line (HEK294) or human embryonic fibroblasts, which are not host cell targets *in vivo*. Just recently, Acott *et al*. [10] utilized Vero cells as a model cell line to establish primary and chronic BKV infection *in vitro*.

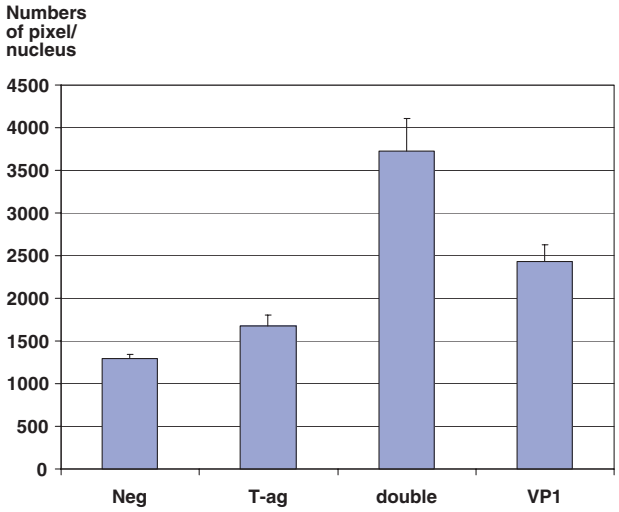

Fig. 3. Correlation of the nuclear size with expression of early and late phase BKV protein. On the *Y*-axis the numbers of pixels are given corresponding to the nuclear size, on the *X*-axis the different phases of the BKV cycle with respect to the expression of large T-antigen and VP1. Bars represent the mean and standard error (SE) of pooled nuclear measurement in all three patients (A, B and C). The nuclear size increases significantly with the course of the virus infection and reaches a maximum upon expression of VP1 in the late replication phase (Wilcoxon test: negative versus T-antigen, versus double versus VP1 $= P < 0.02$, $P < 0.003$, $P < 0.0001$, T-antigen versus double versus VP1 $= P < 0.003$, $P < 0.003$, double versus VP1 $P < 0.05$).

In all of our three cases with PVAN (stages A, B and C), virions were released after cell necrosis and not apoptosis, since activated caspase 3 was absent in infected cells and no nuclear alterations, such as nuclear shrinkage or apoptotic bodies, consistent with ongoing apoptosis, were seen by Hoechst dye. Supporting this concept, CK22 was also strongly expressed in virus-infected cells without any evidence for degradation of the cytoskeleton, typical for apoptosis.

This appears to be in contrast to animal studies of renal-transplanted cynomolgus monkeys with reactivation of the cynomolgus polyoma virus. Here, however, apoptosis affected smooth muscle cells of the ureter and cells of the small intestine. These differences may be explained by the differences in cell type, and by species differences between host and virus.

Our results are consistent with reports by Drachenberg [16] and Nickeleit [17], who analysed the ultrastructural features of BKV nephropathy and described BKV-dependent necrosis in tubular infected cells as the main mechanism of viral lysis.

(2) Utilizing double labelling techniques, our study with three patients in three different stages of PVAN demonstrated a remarkable overlap of large T-antigen and p53 expression. About 70% of large T-antigen positive cells co-stained with p53. In 96% of p53 expressing tubular cells, a complete overlay with T-antigen in the nucleus was detected.

Our findings are in accordance with a recent study from Weinreb *et al*. [18] showing expression of p53 in tubular cells or bladder mucosa of renal-transplanted

patients within cells revealing cytopathic changes or viral intranuclear inclusions. Expression of T-antigen was demonstrated on consecutive sections, but not by double labelling. Accordingly, our study clearly confirms the association of p53 and T-antigen and provides, in addition, the precise number of cells co-expressing T-antigen and p53 in PVAN.

Furthermore and intriguingly, 60% of T-antigen positive cells co-stained for the cell cycle-associated protein Ki67. Therefore, we assume that in the course of the BKV infection first T-antigen is expressed, then T-antigen accumulates and inhibits p53 in the nucleus and finally the cell cycle is activated, as can be seen by the Ki67 expression.

Our data give rise to the hypothesis that *in vivo* similar viral mechanisms control the key cell cycle checkpoint at the G1 to S phase transition, via inhibition of p53 to un-couple the cell cycle. *In vitro*, BKV T-antigen binds readily to the p53 protein in the cell, thereby inducing growth factor independence, but is, by itself, insufficient to allow anchorage-independent growth [19]. Many studies have addressed the process of neoplastic transformation by T-antigen in rodents or human cell culture systems [20]. In our study, we investigated the natural course of BKV infection *in vivo* in renal allografts and provide evidence that similar p53 accumulation mechanisms are operative utilizing most likely wild type p53. *In vitro* data demonstrate that BKV T-antigen binds also to the members of the retinoblastoma family of molecules, thereby affecting cellular growth control [19]. Over-expression of a wild-type p53 has been reported in the case of metastasizing urothelial carcinoma, which was restricted to large T-antigen co-expression and presumably binding [21].

(3) Irrespective of the stage, all our three selected cases revealed the same overlap of expression between T-antigen and p53 and a virtually exclusive T-antigen and VP1 expression. Based on these data, we would like to make a rough hypothetical estimate of the length of the BKV life cycle *in vivo* (Figure 4). However, this appears to be necessarily preliminary since only three cases have been investigated. Assuming that the induction and binding of p53 by T-antigen would last 3 h [22], which would correspond to the biological minimal induction time of p53 by other noxae (e.g. ionizing irradiation [23]), we could calculate from the 70% overlay of p53 and T-antigen a T-antigen expression period of 10 h (Figure 4). The 20% overlay of VP1 expression and T-antigen would correspond to 2 h co-expression of the viral proteins. Consecutively, VP1 would be expressed for an additional 8 h finally resulting in the lysis of the infected cell. All together, from the start of T-antigen expression to virus-dependent lysis, ∼16 h are estimated. Taking into account that the period between virus reception and first viral transcriptional activity would last 24–36 h, as described by Low *et al*., we arrive at a virus life cycle of 40–52 h.

Intriguingly, this time frame is fully in line with the data from Low *et al*. [11] when infecting *in vitro* renal tubular epithelial cells with BKV and detecting progeny virus after 48 h. It is noteworthy, strictly speaking, that the time frame between virus uptake and transcriptional activity given by Low *et al*. is only valid for the primary infection and could differ in cases of reactivating BKV. Our data, however, support the view that, after expression of T-antigen and activation of the virus transcriptional machinery, BKV is released within the same time limits as for the primary infection, also indicating that novel infection of tubular cells after reactivation occurs within similar time frames.

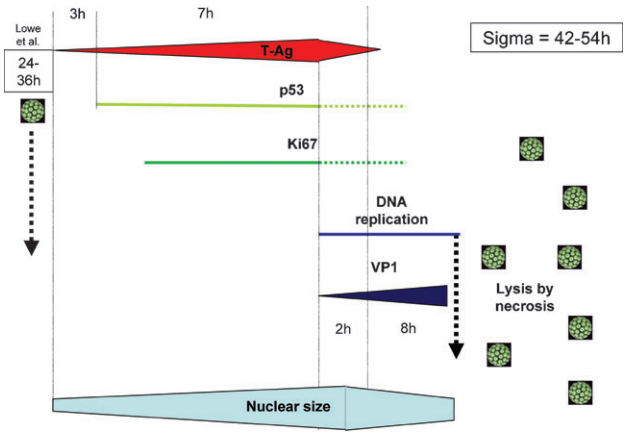

Fig. 4. Estimation of the duration of the BKV infectious cycle *in vivo*. Assuming that the action of BKV T-antigen of p53 binding is a direct effect, a minimal induction time of p53 of 3 h could be assumed (see the Discussion section). From the 70% overlay of p53 and T-antigen a T-antigen expression period of 10 h is assessed. The 20% overlay of VP1 expression and T-antigen would correspond to 2 h co-expression of the viral proteins. Consecutively, VP1 would be expressed for an additional 8 h resulting finally in the lysis of the infected cell. Taking into account that the time between virus reception and first viral transcriptional activity would last 24–36 h as described by Low *et al*. [11] we arrive at a virus life cycle of 42–54 h.

(4) The Ki67 staining was found in tubular epithelial cells with and without large T-antigen expression. Although the presence of episomal viral DNA in these cells cannot be excluded (BKV infected), significant virus replication does not occur in these cells. Most likely, these proliferating cells correspond to cells repopulating the virus-mediated denudation zones as seen under the light microscope. Ki67-positive cells also staining positive for large T-antigen could either be a subpopulation previously infected or now preferentially infected upon Ki67 expression, which now enter the early phase of the viral replication cycle. Alternatively, Ki67 is actually recruited by, and thus a consequence of, large T expression.

(5) Neither the expression of large T-antigen nor of VP-1 was associated with the apoptosis-associated marker caspase-3, indicating that virus-mediated cell loss in PVAN was due to cytopathic replication and cell lysis and not due to apoptosis. Therefore, necrosis with the corresponding inflammatory response seems to be a primary cytopathologic effect. It is not clear whether T-antigen expression *in vivo* is sufficient to mediate anti-apoptotic effects. The negative staining results with bcl-2 suggest that the lack of apoptosis might not be due to over-expression of bcl-2 that is seen in certain malignancies.

In summary, the data from our group of selected patients show that, also in human renal transplants with ongoing PVAN, a clear distinction between early and late phase BKV infection can be made according to the expression of large T-antigen or VP1 protein. Virus-dependent effects appear to be mediated by T-antigen inhibiting p53

and thereby uncoupling the cell cycle. Nuclear enhancement goes hand in hand with the progression of the infectious cycle. Finally, virus-dependent cell death of tubular epithelial cells is necrosis and not apoptosis. Accordingly, we assume that in the inflammatory setting of PVAN, similar BKV mechanisms are operative as in certain *in vitro* systems.

Conflict of interest statement. None declared.

References

1. Gardner SD, Field AM, Coleman DV *et al*. New human papovavirus (BK) isolated from urine after renal transplantation. *Lancet* 1971; 1: 1253–1257
2. Binet I, Nickeleit V, Hirsch HH *et al*. Polyomavirus disease under new immunosuppressive drugs: a cause of renal graft dysfunction and graft loss. *Transplantation* 1999; 67: 918–922
3. Nickeleit V, Hirsch HH, Binet IF *et al*. Polyomavirus infection of renal allograft recipients: from latent infection to manifest disease. *J Am Soc Nephrol* 1999; 10: 1080–1089
4. Purighalla R, Shapiro R, McCauley J *et al*. BK virus infection in a kidney allograft diagnosed by needle biopsy. *Am J Kidney Dis* 1995; 26: 671–673
5. Randhawa PS, Finkelstein S, Scantlebury V *et al*. Human polyoma virus-associated interstitial nephritis in the allograft kidney. *Transplantation* 1999; 67: 103–109
6. Nickeleit V, Singh HK, Mihatsch MJ. Latent and productive polyomavirus infections of renal allografts: morphological, clinical, and pathophysiological aspects. *Adv Exp Med Biol* 2006; 577: 190–200
7. Randhawa P, Brennan DC. BK virus infection in transplant recipients: an overview and update. *Am J Transplant* 2006; 6: 2000–2005
8. Comoli P, Binggeli S, Ginevri F *et al*. Polyomavirus-associated nephropathy: update on BK virus-specific immunity. *Transpl Infect Dis* 2006; 8: 86–94
9. Hirsch HH, Brennan DC, Drachenberg CB *et al*. Polyomavirus-associated nephropathy in renal transplantation: interdisciplinary analyses and recommendations. *Transplantation* 2005; 79: 1277–1286
10. Acott PD, O'Regan PA, Lee SH *et al*. Utilization of vero cells for primary and chronic BK virus infection. *Transplant Proc* 2006; 38: 3502–3505
11. Low J, Humes HD, Szczypka M *et al*. BKV and SV40 infection of human kidney tubular epithelial cells *in vitro*. *Virology* 2004; 323: 182–188
12. Seemayer CA, Kuchen S, Kuenzler P *et al*. Cartilage destruction mediated by synovial fibroblasts does not depend on proliferation in rheumatoid arthritis. *Am J Pathol* 2003; 162: 1549–1557
13. Drachenberg CB, Papadimitriou JC, Hirsch HH *et al*. Histological patterns of polyomavirus nephropathy: correlation with graft outcome and viral load. *Am J Transplant* 2004; 4: 2082–2092
14. Maraldi NM, Barbanti-Brodano G, Portolani M *et al*. Ultrastructural aspects of BK virus uptake and replication in human fibroblasts. *J Gen Virol* 1975; 27: 71–80
15. Seehafer JG, Weil R. Synthesis of polyoma virus structural polypeptides in mouse kidney cells. *Virology* 1974; 58: 75–85
16. Drachenberg CB, Papadimitriou JC, Wali R *et al*. BK polyoma virus allograft nephropathy: ultrastructural features from viral cell entry to lysis. *Am J Transplant* 2003; 3: 1383–1392
17. Nickeleit V, Singh HK, Mihatsch MJ. Polyomavirus nephropathy: morphology, pathophysiology, and clinical management. *Curr Opin Nephrol Hypertens* 2003; 12: 599–605
18. Weinreb DB, Desman GT, Burstein DE *et al*. Expression of p53 in virally infected tubular cells in renal transplant patients with polyomavirus nephropathy. *Hum Pathol* 2006; 37: 684–688
19. Harris CC. Structure and function of the p53 tumor suppressor gene: clues for rational cancer therapeutic strategies. *J Natl Cancer Inst* 1996; 88: 1442–1455
20. Tognon M, Corallini A, Martini F *et al*. Oncogenic transformation by BK virus and association with human tumors. *Oncogene* 2003; 22: 5192–5200
21. Geetha D, Tong BC, Racusen L *et al*. Bladder carcinoma in a transplant recipient: evidence to implicate the BK human polyomavirus as a causal transforming agent. *Transplantation* 2002; 73: 1933–1936
22. Harris KF, Christensen JB, Radany EH *et al*. Novel mechanisms of E2F induction by BK virus large-T antigen: requirement of both the pRb-binding and the J domains. *Mol Cell Biol* 1998; 18: 1746–1756
23. Seemayer CA, Kuchen S, Neidhart M *et al*. p53 in rheumatoid arthritis synovial fibroblasts at sites of invasion. *Ann Rheum Dis* 2003; 62: 1139–1144

Received for publication: 2.7.08
Accepted in revised form: 25.7.08